

## Observation and Analysis of Hydro-morphologic Parameters in Las Glorias beach, México

Cuauhtémoc Franco-Ochoa<sup>1</sup>

Fernando García-Páez<sup>2</sup>

Wenseslao Plata-Rocha<sup>3</sup>

Miguel Montoya-Rodríguez<sup>4</sup>

Miguel Vergara-Sánchez<sup>5</sup>

<sup>1</sup>Universidad Autónoma de Sinaloa, Culiacán, México, cfrancoo@uas.edu.mx, ORCID: <https://orcid.org/0000-0002-7554-3603>

<sup>2</sup>Universidad Autónoma de Sinaloa, Culiacán, México, garpaez@uas.uasnet.mx

<sup>3</sup>Universidad Autónoma de Sinaloa, Culiacán, México, wenses@uas.edu.mx

<sup>4</sup>Instituto Mexicano del Transporte, Querétaro, México, mmontoya@imt.mx

<sup>5</sup>Instituto Politécnico Nacional, Ciudad de México, México, mvergara@ipn.mx

Correspondence author: Cuauhtémoc Franco Ochoa, email: cfrancoo@uas.edu.mx

### Summary

Based on measurements and sampling carried out quarterly along 18 profiles of the Las Glorias beach from August 2015 to May 2016 and with the wave data provided by the Mexican Institute of Transport (IMT), on the one hand, the changes in the profile of the beach and its relationship with the wave regime impacting it are analyzed and, on the other hand, a database is provided that includes the analysis of swell, sediment and morphology data for future studies on its morph dynamics. The results revealed that the distribution of sediments on the beach is spatially and temporally very homogeneous and that the inter-annual cycle of change of the beach profile responds to the seasonal wave regime.

**Keywords:** beach profile, Las Glorias beach, waves, morphology.

### **Abstract**

The aim of this study was to provide and analyze swell, sediment and morphology data of the Las Glorias beach, which on one hand allows determining the variability of the beach profile and its relationship with the wave regime, and on data including sedimentology for further morph dynamics studies. The sediment and morphology data of Las Glorias beach were collected along eighteen beach profiles quarterly, from august 2015 to May 2016, and the IMT provided wave data. The results show that the distribution of sediments on the beach is very homogeneous and the changes in the beach profile correspond clearly to the seasonal variation of the waves.

**Keywords:** beach profile, Las Glorias Beach, waves, morphology.

Recieved: 13/01/2018

Accepted: 08/08/2018

## Introduction

Las Glorias beach is located in the Gulf of California on the coast of the State of Sinaloa, between meridians 747 000 m and 753 000 m and the parallels 2 798 000 m and 2 802 000 m of the zone 12 north of the UTM system (Figure 1). It has an approximate extension of 5 km. It is limited at its ends by rock breakwaters. Its morphology as seen from above is practically straight, with parallel bathymetry. Two hydrological basins discharge towards the beach: the Sinaloa river basin and the Bahía Lechuguilla - Ohuira - Navachiste basin. The climate is arid and semi-arid with rains mainly in the summer (García, 2004). On the beachfront, occur mixed astronomical tides with semi-diurnal predominance (SMN, 2018), that is, two high tides and two low tides occur during each lunar day, and the levels of two consecutive high tides or low tides are generally similar. The amplitude of these tides is located in the micromareal range (less than 2 m) according to the Davies classification (1964).

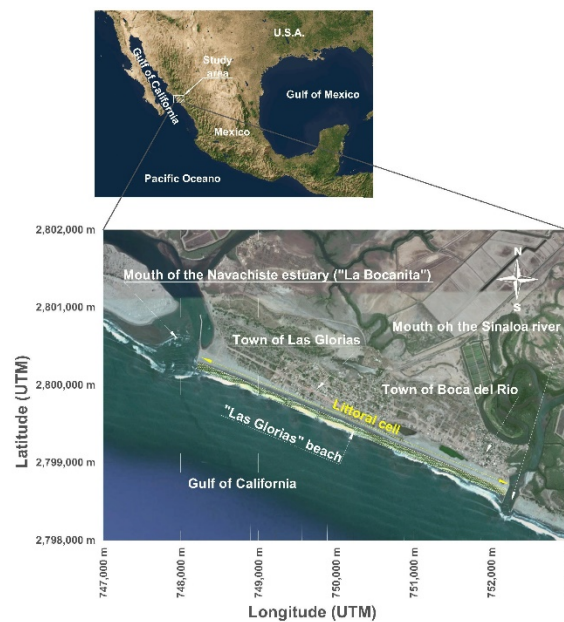


**Figure 1.** Location of "Las Glorias" beach, Sinaloa.

According to Alcántar (2007), in the 80's it was possible to observe the formation of sand arrows in front of the mouths of the Sinaloa river and the Navachiste estuary, due to the interaction between waves, currents and coastal transport. The arrow in front of the Sinaloa River caused the river to change its course towards the northwest and to end at approximately the middle of Las Glorias beach. In the same decade, the Lic. Gustavo Díaz Ordaz and Lic. Guillermo Blake Aguilar dams were completed on the Sinaloa river beds and on its main tributary, the Oconori stream, respectively, which caused a drastic reduction in the sediment supply to the beach, resulting in a sedimentary decompensation which began the erosion of the beach. Later, at the beginning of the 90's, a canal was dredged on the beach with the purpose of relocating the mouth of the Sinaloa River to the southeast. At the same time two rock-based breakwaters were built with the purpose of horizontally stabilizing said outlet. Consequently, on the one hand, in the back of the beach small lagoons were formed as a result of the old bend of the Sinaloa River, and on the other, a physical barrier was generated that interrupted the passage of coastal sediment transport to the Las Glorias beach side. This aggravated its sedimentary decompensation. Regarding changes in the beach coastline, Alcántar (2007) estimated that this fell back 149 linear meters between 1980 and 2004, with an average erosion rate of 6.2 m / year. Finding that the highest rate of erosion occurred between 1990 and 1994, this being 9.2 m / year, erosion that could be associated with the construction of breakwaters at the mouth of the Sinaloa River in 1992 and 1993. As for the profiles, reports that the erosion occurs in summer, while accretion occurs in the winter.

With the years some actions focused on the restoration and recovery of the Las Glorias beach have been carried out, the most important were carried out in 2006, which consisted of a beach nourishment in a 2 km extension, an average width of 71.50 m, with an elevation of +1.0 m above the Mean Low Water (MLW) and the construction of a breakwater at the mouth of the Navachiste estuary, although it was designed for a length of 311.90 m, only 146.90 m were built (Limón, 2010). Regarding

the response of the beach to these works, Zayas (2010) reported that between 2003 and 2008 there was both an advance and retreat of the beach coastline. In general, the coastline advanced northwest of the beach due to the accumulation of sediments in the breakwater, while in the rest of the beach the coastline receded mainly in the area of construction.

According to this, it is concluded that the beach is under considerable conditions of anthropogenic alteration, mainly by the construction of engineering works both on the beach and in the Sinaloa River, observing an advanced state of deterioration due to the erosion impacting said anthropic alteration.

Given the unstable situation of the beach, the need to establish measures for its restoration and recovery is evident, and therefore a detailed study to understand the degree of balance it maintains and the processes involved in it. In this regard, the present study is focused on providing and analyzing beach swell, sediment and morphology data, which on the one hand will allow us to understand the relationship between the temporal change of the shape of the beach profile and the wave dynamics that involve sediment transport and, on the other hand, provide a basis for further studies on its morph dynamics.

## **Methodology**

### **Acquisition and statistics of wave data**

The wave information analyzed in this work corresponds to the PAC17MX node located at 25° north latitude and 109° west longitude of the Mexican Oceanic Wave Atlas (ATLOOM) of the Mexican Institute of Transport (IMT). This Atlas was generated using the WAMC4 wave model with meteorological information from the National Center for Environmental Prediction (NCEP) and National Center for Atmospheric Research (NCAR) agencies, which generated 44 years of swell information in the deep-water region along the Mexican coast (from January 1, 1958 to December 31, 2001) and the results obtained were compared and validated with the information recorded by directional buoys of the National Data Buoy Center (NDBC) (Montoya, 2016).

The analysis of wave patterns was carried out after classifying the data by season (summer, autumn, winter and spring). Table 1 shows the months that were considered to define each season, as well as the number of data included.

**Table 1.** - Months considered to define the different seasons of the year and the number of data included in each one of them.

Season	Months considered	No. of data
Summer	June - August	99182
Autumn	September - November	93783
Winter	December - February	89789
Spring	March - May	97006
Total		379760

To characterize tide-waves by height, period, direction and frequency of occurrence, height and period wave roses were generated. Also, the following statistical parameters of the swell were evaluated: average height ( $\bar{H}$ ), average period ( $\bar{T}$ ), middle address ( $\bar{\theta}$ ) and the 50th percentiles ( $H_{50}$ ) and 100 ( $H_{100}$ ) of wave height.

## Refraction and subtraction

The Orthogonal Method was applied to calculate the wave transformation by refraction and subtraction described in the Coastal Engineering Manual of the Army Corps of Engineers of the United States of America (Vincent, Demirbilek, & Weggel, 2002). This for the purpose of estimating the magnitude of the heights and orientation of the waves in the shallow water region at the beach front, based on the deep sea wave information from ATLOOM.

Wave height transformed at a particular point in shallow water ( $H_1$ ), is calculated as:

$$H_1 = H_0 \times K_s \times K_r$$

Where,  $H_0$  is the height of the wave in deep water,  $K_s$  is the coefficient of subtraction and  $K_r$  is the refraction coefficient.

The coefficient of subtraction  $K_s$  is calculated as:

$$K_s = \left( \frac{C_{go}}{C_{gl}} \right)^{\frac{1}{2}}$$

Where,  $C_{go}$  and  $C_{gl}$  are wave group speeds for deep and transitional waters, respectively, and are calculated as:

$$C_{go} = \frac{1}{2} \left( \frac{gT}{2\pi} \right) \quad \text{and} \quad C_{gl} = \frac{1}{2} \left[ 1 + \right.$$

$$\left. \frac{4\pi d/L}{\sinh(4\pi d/L)} \right] \left( \frac{gT}{2\pi} \tanh \left( \frac{2\pi d}{L} \right) \right)$$

Here,  $g$  is the gravity,  $T$  denotes the wave period,  $L$  is the wave length at a particular location, and  $d$  represents the depth of the water.

On the other hand, the refraction coefficient is calculated as:

$$K_r = \left( \frac{1 - \sin^2 \theta_0}{1 - \sin^2 \theta_1} \right)^{\frac{1}{4}}$$

Where,  $\theta_0$  is the angle of incidence in deep water (direction of the wave),  $\theta_1$  is the angle of incidence at a particular place in shallow water. Since the swell, under certain approaches complies with Snell's Law, it can be stated that:

$$\frac{\sin \theta_1}{C_1} = \frac{\sin \theta_0}{C_0}$$

Here,  $C_1$  and  $C_0$  are the wave speed in shallow and deep water, respectively, and are calculated as

$$C_1 = \frac{L}{T} \quad \text{and} \quad C_0 =$$

$$\frac{gT}{2\pi}$$

Therefore, the angle of incidence at a particular location in shallow water is calculated with an equation derived from Snell's Law and equals:

$$\theta_1 = \sin^{-1} \left( \frac{C_1 \times \sin \theta_0}{C_0} \right)$$

## Measurement of beach profiles

For the measurement of the beach profiles, geodesic control points were established by means of satellite measurements in static mode with dual frequency GPS receivers to link the topo - bathymetric points to the active national geodesic network (RGNA) of the National Institute of Statistics and Geography (INEGI, 2010), particularly at the apex of Culiacán.

In this way, the geodesic points of horizontal and vertical support were established, with their geodesic and known UTM coordinates, as well as their elevation above the Mean Sea Level (MSL) that allowed, through the transverse sectioning of the coastline, to obtain the characterization of the main elements that, according to Carranza & Caso (1994), make up the profile of the beach.

To achieve this characterization, the elevations of the natural terrain along the beach profile were measured with varying distances of between 5 and 20 m, depending on the changes in slope of the relief, which goes from the upper limit on the ground of the beach to the breakers area, usually during low tide, to cover a greater length of beach. Such measurements were obtained using an electronic tachymeter (total station) and stick prisms, that is, by tachymetry or trigonometric leveling, and do not include the part of the beach profile that goes beyond the swell zone in the direction of the sea.

The separation between successive beach profiles was approximately 250 m, giving a total of 18 profiles (Figure 2).

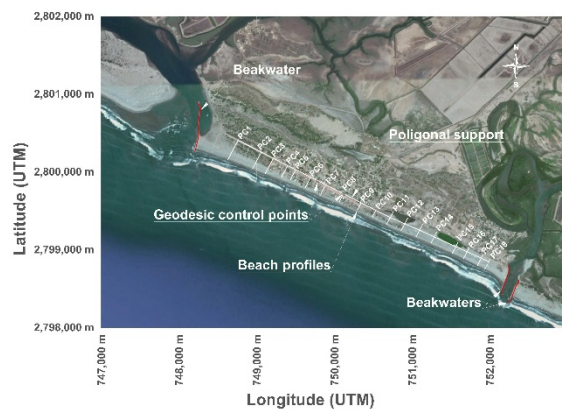


**Figure 2.** Location of beach profiles.

The processing of the information obtained from both GPS and tachymetric measurements was processed by rigorous geodesic and topographic methods, in specialized software with equipment - computer interface to obtain control point and cross section information in the ITRF2008 Global Reference System and in the Universal Transverse Mercator (UTM) cartographic projection. Once the digital file of points

was obtained, the cartographic drawing was carried out in Autocad®, Civilcad® and Matlab® software to obtain the coastline and the beach profiles.

## Sediment sampling

Sediment samples were collected along the beach profiles in Figure 2. The profile elements from which they were collected were: the upper limit of the beach (berm or dune), and the swept and traverse zones. The samples were approximately 2 kilograms and were taken superficially. A total of 198 samples were collected, and they were performed at the same time as the measurement of the profiles.

Granulometry was performed on each sample collected by a mechanical sieve method. The selection of the set of sieves was made so that they were conveniently spaced according to the distribution of sediment sizes. Also, some textural parameters of the sediments were estimated, such as: average size ( $D_m$ ), standard deviation ( $\sigma$ ), bias ( $SkI$ ) and kurtosis ( $KG$ ).

## Results

From the body of data from waves in deep waters it was observed that in all the seasons of the year the highest frequencies of occurrence correspond to waves with wave heights within the intervals of 0.5 to 1.0 m and 1.0 to 1.5 m with periods between 6 and 12 s, mainly from the south and southwest  $22.5^\circ$  (figure 3). Likewise, the highest values for spring and summer of  $\bar{H}$  and  $H_{50}$  were estimated, which are quite similar, while the lowest values were estimated for winter (table 2). However, the highest value for  $H_{100}$  was estimated for the autumn, followed by summer, spring and winter. Regarding the estimated values of  $\bar{T}$ , they were found to be low and showed little seasonal variability.

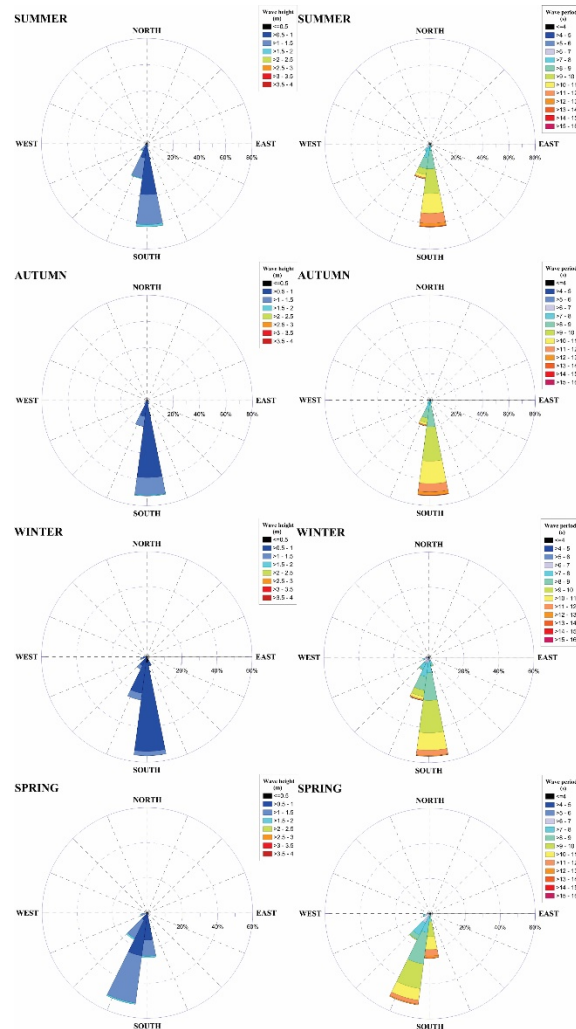


**Figure 3.** Wave roses for wave height and period by season.

**Table 2.** Estimated values for parameters of deep water swell were evaluated: average height ( $\bar{H}$ ), average period ( $\bar{T}$ ), middle address ( $\bar{\theta}$ ) and the 50th percentiles ( $H_{50}$ ) and 100 ( $H_{100}$ ) of wave height.

Season	$\bar{H}$ m	$H_{50}$ m	$H_{100}$ m	$\bar{T}$ s	$\bar{\theta}$ °
Summer	1.05	1.28	2.66	9.12	189.20
Autumn	0.93	1.09	3.02	9.30	186.18
Winter	0.80	0.97	2.06	8.53	192.15
Spring	1.07	1.30	2.25	8.81	203.00

On the other hand, during the year there was not a significant difference in the waves in shallow water at the beach front in terms of their direction. This predominantly hit the beach practically perpendicular (figure 4 and table 3) . As for their height, it was also quite regular in a range of 1.0 to 1.5 m, except in winter where the heights are lesser, in the order of 0.5 to 1.0 m.

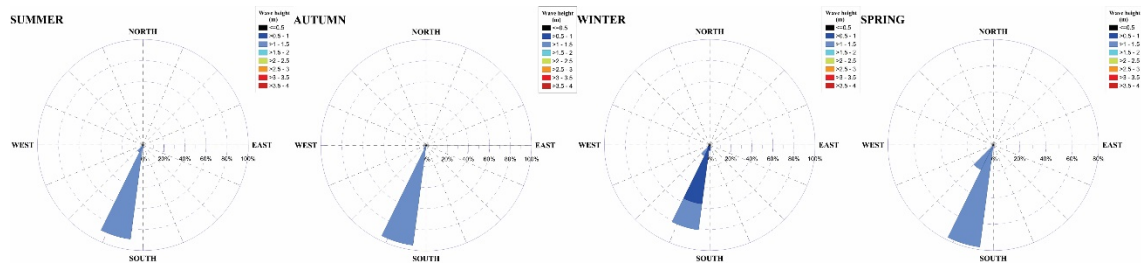


**Figure 4.** Wave roses illustrating waves affected by refraction and subtraction.

**Table 3.** Estimated values of the statistical variables of the waves transformed by refraction and subtraction: average height ( $\bar{H}_R$ ) and mean direction ( $\bar{\theta}_R$ ).

Season	$\bar{H}_R$ m	$\bar{\theta}_R$ °
Summer	1.32	198.94
Autumn	1.17	197.98
Winter	0.97	199.68
Spring	1.33	203.24

Regarding the profile of the beach, it was found that in all the control points the two extreme forms of profile are summer and winter (figure 5). In general, the shape of the slope of the summer profile is more pronounced and with abrupt changes, in contrast, the winter profile

shows a more or less continuous gentle slope, as well as the formation of a berm.

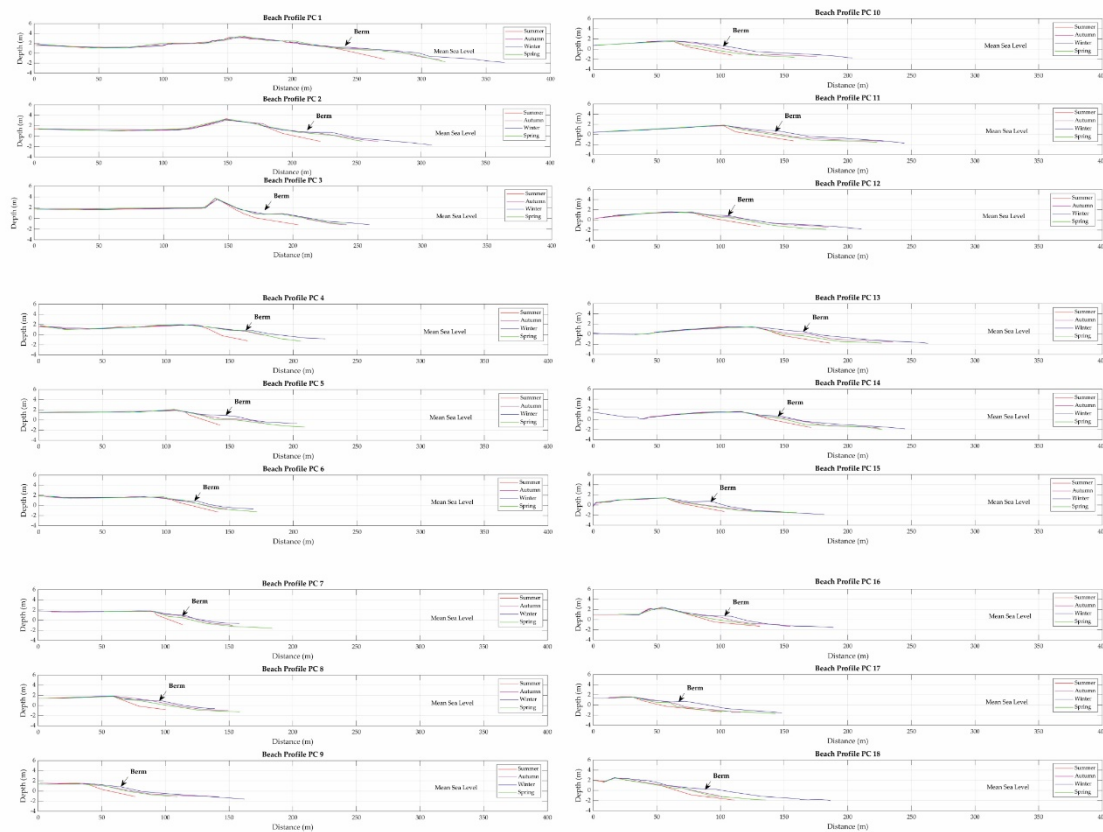


**Figure 5.** Beach profiles of the 18 control points measured quarterly from August (summer) 2015 to May (spring) of 2016.

About the textural parameters of the sediments, these did not vary significantly along the beach or between seasons (table 4), on average they showed a size of  $2.477 \phi$ , a standard deviation of  $0.134 \phi$ , asymmetry of  $-0.145 \phi$  and kurtosis of  $1.364 \phi$  (in Phi ( $\phi$ ) units).

**Table 4.-** Estimated values of the of the sediment textural parameters in units Phi ( $\phi$ ): average size ( $D_m$ ), standard deviation ( $\sigma$ ), bias ( $SkI$ ) and kurtosis ( $KG$ )

Season	$D_m$	$\sigma$	$SkI$	$KG$
Summer	2.453	0.128	-0.163	1.321
Autumn	2.473	0.136	-0.142	1.399

Winter	2.455	0.132	-0.115	1.344
Spring	2.520	0.138	-0.159	1.391

## Discussion

The seasonality of the wave regime is reflected in the changes in the beach profile (figure 5), since it is not the same throughout the year. The estimated values of the statistical parameters of the swell (table 4) indicate that in autumn wave height begins to decrease, in comparison with that observed in summer, until reaching winter swell, while, in spring, wave height increases and remains similar until summer. This behavior causes the profile of the beach to increase from autumn to winter, when the waves decrease in height until they reach low average values, and is eroded from spring to summer, when the waves are higher and more consistent. These changes in the beach profile occurred in virtually all control points along the beach, bearing great resemblance to those reported by Alcántar (2007). However, the inter-annual cycle of change in the Las Glorias beach profile, which consists of phases of erosion and accretion occurring in spring-summer and autumn-winter, respectively, is not reversed as indicated by Alcántar (2007). , because the changes in the morphology of the beach profile respond to changes in wave conditions (Masselink & Hughes, 2003), that is, high-energy waves produce erosion and low-energy produce accretion, as verified in this work.

The swell due to the effect of refraction and subtraction tend to regularize in the beach front in terms of its direction and height (figure 4). Nevertheless, higher waves dominate in spring and summer, while those of lower height dominate in autumn and winter (table 5). As the waves tend to impact, predominantly, practically perpendicularly on the beach in every season of the year, this indicates that little sediment transport occurs longitudinally to the beach, rather the transport of sediment is in transverse direction, that is, the higher waves erode the berm and tend to deposit the sediment in front of the beach in the form of a bar, which is then removed towards the beach by the lower height waves, forming a new berm.

In relation to the textural parameters of the sediments, since these did not vary significantly along the beach or between seasons, their distribution is spatially and temporally very homogeneous. Taking into account the limit values of the textural parameters described in the Coastal Engineering Manual of the Army Corps of Engineers of the United States of America (King & Galvin, 2002) the sediments consist of very well classified fine sand, which is asymmetric towards thick and leptocurtic sizes. The homogeneity of the type of sediment suggests that it has a lower relative influence than the swell on the changes to the beach profile.

## Conclusions

Higher waves dominate in spring and summer, while those of lower height dominate in autumn and winter. However, in autumn, the highest waves of the year occur; a condition where the beach can change its profile in a very short time.

Beach profiles show morphological changes with a marked seasonality, it can be observed that the maximum accretion is in winter and the maximum erosion in summer, this verifies that the inter-annual cycle of change of the beach profile responds to the seasonal regime of the swell.

The presence of a berm is typical of winter and the slope of the beach as a whole is lower than during the other seasons; On the contrary, the absence of the berm and the greater slope of the beach are typical of summer.

The distribution of the sediment that comprises the beach is spatially and temporally very homogeneous, fine sands predominate.

### **Acknowledgments**

The Mexican Institute of Transport (IMT) is thanked for sharing the wave data used to prepare this work.

### **References**

Alcántar, R. (2007). *Variabilidad espacio temporal del perfil de playa, en playa Las Glorias en Guasave, Sinaloa*. Tesis de Maestría. Guasave, Sinaloa: Instituto Politécnico Nacional.

Carranza, E., & Caso, M. (1994). Zonificación del perfil de playa. *Revista Geo-UNAM*, 2, 26-32.

Davies, L. (1964). A morphogenic approach to world shorelines. *Zeitschrift für Geomorphologie*, 8, 27-42.

García, E. (2004). *Modificaciones al sistema de clasificación climática de Köppen*. Ciudad de México: Universidad Nacional Autónoma de Sinaloa. Recuperado de [http://www.igeograf.unam.mx/sigg/utilidades/docs/pdfs/publicaciones/geo\\_siglo21/serie\\_lib/modific\\_al\\_sis.pdf](http://www.igeograf.unam.mx/sigg/utilidades/docs/pdfs/publicaciones/geo_siglo21/serie_lib/modific_al_sis.pdf)

INEGI (2010). *Red Geodésica Nacional Activa*. Ciudad de México: Instituto Nacional de Estadística y Geografía. Recuperado de <http://www.inegi.org.mx/geo/contenidos/geodesia/coordenadas2010.aspx>

King, D., & Galvin C. (2002). Coastal Sediment Properties (III-1-1-III-1-41). *Coastal Engineering Manual*. Washington, DC: U.S. Army Corps of Engineers. Recovered from [https://www.publications.usace.army.mil/Portals/76/Publications/EngineerManuals/EM\\_1110-2-1100\\_Part-03.pdf?ver=2014-03-10-134006-163](https://www.publications.usace.army.mil/Portals/76/Publications/EngineerManuals/EM_1110-2-1100_Part-03.pdf?ver=2014-03-10-134006-163).

Limón, J. (2010). *Manifestación de impacto ambiental, modalidad particular para el proyecto de: escolleras, protección marginal playera y dragado del canal de acceso en la Bocanita, municipio de Guasave, Sinaloa*. Recuperado de <http://sinat.semarnat.gob.mx/dgiraDocs/documentos/sin/estudios/2010/25SI2010H0009.pdf>

Masselink, G., & Hughes, M. (2003). *Introduction to coastal processes and geomorphology*. Euston Road, London: Hodder Education.

Montoya, M. (2016). Red Nacional de Datos Oceanográficos para Zonas Costeras. *Revista IC Ingeniería Civil*. 566, 14-18. Recuperado de [https://issuu.com/helios\\_comunicacion/docs/ic-566\\_ok/16](https://issuu.com/helios_comunicacion/docs/ic-566_ok/16).

SMN (2018). *Servicio Mareográfico Nacional*. Ciudad de México: Instituto de Geofísica, Universidad Nacional Autónoma de México. Recuperado de <http://www.mareografico.unam.mx/portal/index.php?page=tiposMarea>

Vincent, L., Demirbilek, Z., & Weggel, R. (2002). Estimation of Nearshore Waves (II-3-1-II-3-41). *Coastal Engineering Manual*. Washington, DC: U.S. Army Corps of Engineers. Recovered from [http://www.publications.usace.army.mil/Portals/76/Publications/EngineerManuals/EM\\_1110-2-1100\\_Part-02.pdf?ver=2016-02-11-153511-290](http://www.publications.usace.army.mil/Portals/76/Publications/EngineerManuals/EM_1110-2-1100_Part-02.pdf?ver=2016-02-11-153511-290)

Zayas, E. (2010). *Efectos en playas Las Glorias causados por la construcción del espigón al modificar el transporte litoral*. Tesis de Maestría. Guasave, Sinaloa: Instituto Politécnico Nacional.